Applying Differentiated Retinal Cell for Age-Related Macular Degeneration Treatment

Shahmoradi, Saleheh; Yazdian, Fatemeh*+

Department of Life Science Engineering, Faculty of New Sciences and Technologies, University of Tehran, Tehran, I.R. IRAN

Janghorbani, Amin

Department of Biotechnology, Faculty of New Sciences and Technologies, Semnan University, Semnan, I.R. IRAN

Satrian, Leila; Behroozi, Farnaz

Department of Stem Cells and Developmental Biology, Cell Science Research Center, Royan Institute for Stem Cell Biology and Technology, ACECR, Tehran, I.R. IRAN

Tabandeh, Fatemeh

Bioprocess Engineering Group, Industrial and Environmental Biotechnology Department, National Institute of Genetic Engineering and Biotechnology (NIGEB), Tehran, I.R. IRAN

Navaei-Nigjeh, Mona

Pharmaceutical Sciences Research Center, The Institute of Pharmaceutical Sciences (TIPS), Tehran University of Medical Science, Tehran, I.R. IRAN

ABSTRACT: *Age-related Macular Degeneration (AMD) is one of the retinal degenerative diseases associated with some degree of dysfunction and loss of Retinal Pigmented Epithelium (RPE) cells and leads to permanent sight loss. Available treatments only slow down its progression. Applying a scaffold to help RPE cells proliferation and make layers has been proposed as a promising approach to treat this group of diseases. In this study, a fuzzy system was used to optimize the situation of making a scaffold. For better adhesion and proliferation of cells, the polycaprolactone scaffold's surface was modified by alkaline hydrolysis and plasma. Some analyses, such as water uptake and biodegradation rate, were done. Then, differentiated human embryonic stem cells (hESCs) were cultured on several groups of scaffolds. Finally, the viability, proliferation, and morphology of differentiated hESC-RPE cells on all groups of the scaffolds were investigated. The nanofibers' diameter was minimized by optimizing voltage and solution concentration with a fuzzy model for the first time, which obtained 110.5 nm, 18.9 kV, and 0.065 g/mL (w/v), respectively. The immersion time of the scaffold in alkaline solution and solution concentration during surface modification were achieved 4.3 M and 104 minutes, respectively, by response surface methodology. Results of the MTT assay showed that the hydrolyzed group had a high proliferation of cells. Scanning electron microscopy observation of cell morphology after 60 days confirmed this result. In conclusion, our results demonstrate that the hydrolyzed scaffold is a suitable bed for cell proliferation, a good option for AMD treatment.*

KEYWORDS: *Age-related macular degeneration; Polycaprolactone; Optimization; hESCs; Fuzzy model.*

INTRODUCTION

Age-related macular degeneration (AMD) is one of the age-related diseases of the retina, which leads to blindness in the elderly (over 65 years of age) population worldwide [1, 2]. In AMD, retinal pigment epithelium (RPE) cells -a pigmented cell monolayer that supports the photoreceptors and sits on a pentalaminar sheet called Bruch's membrane (BM)- are degraded irreversibly [3–5]. The fibers' diameter of BM range from 50 to 500 nm and the membrane's thickness is less than 5µm. BM helps RPE cells maintain their monolayer structure and transfer nutrients and metabolites to and from choriocapillaris located on the other side of BM [6]. Unlike fish and amphibians, mammals can't regenerate the damaged retina [7, 8].

Human embryonic stem cells (hESCs) are a promising source of RPE cells for treating common and incurable forms of severe visual impairment, such as AMD [9, 10]. In tissue engineering, using a scaffold as a bed to proliferate and differentiate cells has gained huge attention nowadays [11]. The scaffold consists of nanofibers that help cells proliferate and make a layer to substitute the disrupted RPE layer [12, 13]. Scaffolds show the advantages of surface topology in nanoscale and induce desirable cellular responses. Nanoscale topological cues can influence the morphology and differentiation of cell types [14].

Pennington et al. believed that the culture of stem cell-derived RPE monolayers on scaffolds is an excellent approach for treating AMD and other retina diseases. Pluripotent stem cells can potentially be used as an unlimited source of RPE cells [15]. In another study, porous honeycomb-like films were used as scaffold materials for human embryonic stem cell-derived RPE (hESC-RPE) cells. A high permeable film with dip-coating of collagen type IV fabricated the homogeneous surface. Cells were cultured on this surface and the detection of specific RPE markers confirmed the differentiation of hESC-RPE cells. Since porous honeycomb films enabling the free flow of ions and molecules across the material, they are suggested for application in hESC-RPE tissue engineering [16]. Additionally, in a study, polybutylene succinate (PBSU) films were used as a polymeric surface to support hESC-RPE cells' adhesion. Results showed that the films' physical properties and biocompatibility are highly dependent on the adopting casting method [17].

different polymers are used to fabricate scaffolds, such as Poly Lactic Acid (PLA), Poly Glycerol Sebacate (PGS) etc. Among them, polycaprolactone (PCL) is used because of its biocompatibility, biodegradability, high tensile strength. Electrospinning of this polymer enables us to make a scaffold with different diameters and porosity. Previous studies showed that the relationship between the voltage of electrospinning, the concentration of the solution, and nanofibers' diameter is nonlinear [18]. A neuro-fuzzy model is a powerful tool that can use the information from experts' knowledge, observations, and data to model the behavior of a system and the relationship between its parameters [19]. Since PCL is a hydrophobic polymer, its surface was modified by alkaline hydrolysis and oxygen plasma to be suitable for cell adhesion and, finally, cell proliferation. After optimizing nanofiber diameter and hydrolysis condition, differentiated hESC-RPE cells were cultured, and some analysis was done to suggest this scaffold as AMD treatment.

In this study, the ANFIS is applied to model the optimized scaffold for the first time. The resulting fuzzy model was used to modify its surface for better cell proliferation. After doing some tests on scaffolds, cell analyses were used to determine the behavior of polymeric scaffold as a choice in AMD treatment.

EXPERIMENTAL SECTION

Preparing scaffold and optimization of scaffold based on diameters

In order to obtain a clear solution, polycaprolactone (PCL) ($M_{n=}$ 80000 Da, Sigma Aldrich Co.) in pellet form was dissolved in dimethylformamide (DMF, Merck Co.) and chloroform (CHL, Merck Co.) with 2:8 volume ratio for 4 hours at room temperature with stirrer [20]. Then the solution was electrospun from a syringe with 10 mm diameter and 3 mL volume with an adjustment of device parameters [18].

Since smaller diameters of nanofibers are ideal for cell culture, after selecting the effective parameters as variables of the electrospinning process, a set of experiments were designed by response surface method (RSM). Voltage and concentration of solution were considered as variables 12.5-22.5 kV and 0.06-0.14 g PCL /mL solvent, respectively [21, 22]. Other parameters were assumed constant, which are shown in Table 1.

Experiments were done and scaffolds fabricated. Finally, by analyzing Scanning Electronic Microscopy (SEM) images of fabricated scaffolds and measuring the

Table 1: Constant parameters fabricating scaffold by electrospinning method.

Parameters	Tip to collector distance (cm)	Solution temperature (c)	Speed of drum (rpm)	Rate of solution (mL/h)
Amount	10	27	750	0.5

diameter of nanofibers by Image J, the optimized condition was obtained using a fuzzy model.

Adaptive neuro-fuzzy inference system (ANFIS) structure

ANFIS , is one of the famous neuro-fuzzy systems, was initiated by Jang in 1993 [23]. This system implements a Takagi-Sugeno fuzzy inference system. Assume that a fuzzy inference system has two input, x_1 and x_2 and one output y. A typical rule-based of Takagi-Sugeno fuzzy inference system with m rule can be expressed as:

Rule#1: if x_1 is A_1 and x_2 is B_1 then: $y_1 = \alpha_1 x_1 + \beta_1 x_2 + \gamma_1$

Rule#2: if x_1 is A_2 and x_2 is B_2 then: $y_2 = \alpha_2 x_1 + \beta_2 x_2 + \gamma_2$

Rule#M: if x_1 is A_m and x_2 is B_m then: $y_m = \alpha_m x_1 + \beta_m x_2 + \gamma_m$

In which A and B are fuzzy membership functions for x_1 and x_2, respectively, and y is the network's output, which is a linear combination of the inputs.

ANFIS structure is comprised of 5 layers [24, 25]:

Layer 1: This layer is the fuzzification layer in which each neuron has a membership function; the output of this neuron is the membership degree of the crisp value of the input to each membership function of the neurons.

Layer 2: the second layer neurons contain a t-norm operator such as product which calculate the product of membership degree of the inputs in their associated fuzzy membership functions as a scale of rule firing strength W_i:

$$W_i = \mu_{A_i}(x_1) \times \mu_{B_i}(x_2) \tag{1}$$

The firing strength rule measures the satisfaction of the antecedent part of a fuzzy rule with the input vector.

Layer 3: the third layer is normalization, which normalizes each rule's firing strengths calculated in the previous layer. The normalized output of this layer ($\overline{W_i}$) is computed as the ratio of each rule firing strength to the sum of all rules firing strength:

$$\overline{W_i} = \frac{W_i}{\sum_{i=1}^{m} W_i} \tag{2}$$

Layer 4: this layer computes the output of each rule based on Eq.3

$$y_i = \overline{W_i}(\alpha_i x_1 + \beta_i x_2 + \gamma_i) \tag{3}$$

Layer 5: this layer calculates the final output of the system with summation of all previous layer outputs

$$y = \sum_{i=1}^{m} y_i = \frac{W_i(\alpha_i x_1 + \beta_i x_2 + \gamma_i)}{\sum_{i=1}^{m} W_i} \tag{4}$$

The structure of the ANFIS is shown in Fig. 1a.

The parameters of the membership functions in the first layer, called antecedent parameters and the parameters of forth layer (α_i, β_i and γ_i), called consequent parameters, must be determined properly to achieve a good modeling performance. These parameters in ANFIS structure are tuned based on observed input-output pairs from the system and a hybrid learning algorithm. The last layer's parameters are tuned based on the least-squares method and the parameters of the first layer are adjusted using gradient descent and backpropagation error algorithm. More details about the hybrid algorithm can be found in [23, 26].

In this study, the three-triangular fuzzy membership function is selected for each input in the first layer and the product is used as the t-norm operator. The input variables of the ANFIS in this study were the electrospinning voltage and the solution concentration. In order to tune the parameters of the ANFIS, 40 input-output pairs were generated during the electrospinning of nanofibers with the variation of the voltage in the range of 12.5-22.5 kV and the concentration of the solution in the range of 0.06-0.14 g PCL /mL solvent. The diameter of the nanofibers was measured as the output of the electrospinning process. To this end, every 40 input-output pairs were used to train the ANFIS parameters using the hybrid learning algorithm. Finally, the resulted fuzzy model was used to estimate the diameter of the nanofibers based on arbitrary values of the electrospinning voltage and the solution concentration. So, the optimum values of these parameters to reach the minimum diameter of nanofibers can be determined based on this model.

Using the achieved fuzzy model showed good agreement between experimental and predicted values of ANFIS model. The coefficient of determination of train
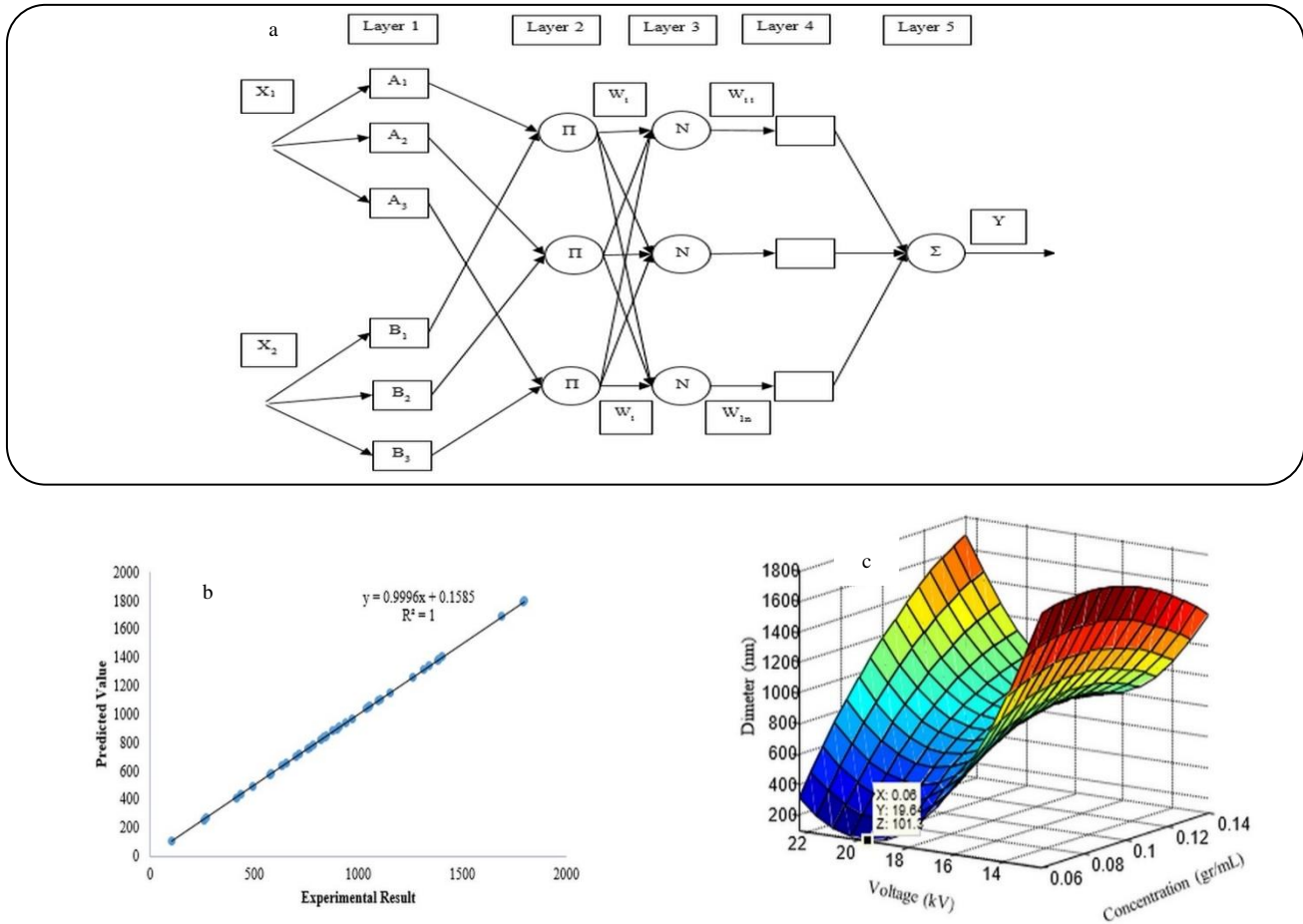
Fig. 1: a) The structure of the ANFIS, b) Predicted values versus experimental results of electrospinning process, c) 3D surface related to nanofiber diameter, solution concentration and voltage. The optimum condition was obtained which was concentration of solution=0.065 g PCL /mL solvent, voltage=18.9 kV and diameter of fibers=110.5 nm.

and test was 1 (Fig. 1b). The generalization performance of the best-fitted surfaces of fuzzy model is illustrated and the optimum condition can be seen in Fig. 1c.

Surface modification and optimization

PCL is a hydrophobic polymer that needs to be hydrophilic to improve cell adhesion and proliferation. Alkaline hydrolysis, a method for increasing the hydrophilicity of PCL, hydrolyses ester bonds and creates hydrophilic carboxylic groups. Hence, sodium hydroxide (NaOH, Merck Co.) was dissolved in distilled water and an alkaline solution was made. A set of experiments was designed to reach the optimized conditions of alkaline solution concentration (with the range of 0.5-6.5 M) and exposure time of scaffolds in alkaline solution (with the range of 30-150 min). Ultimately, treated scaffolds were rinsed three times with distilled water to return pH 7 [22].

Contact angle measurement was used as an evaluation method for finding the optimum condition of the applied alkaline hydrolysis. Four µl volume of deionized water was dropped on the surface of treated scaffolds and the contact angle of water was measured with an optical bench-type contact angle goniometer (Dataphysics, CA 15 plus) [27]. To investigate the effect of simultaneous using of two types of treatment on cell culture, plasma treatment was carried out in low pressure radio frequency (RF) oxygen discharge. So, after hydrolyzing scaffolds some samples were put in chamber and treated at 150 W for 15 min [28].

Porosity, thickness, diameter

SEM (KYKY, EM 3200) was used for the measurement of nanofibers' diameter (with Image J software) and thickness [29].

For determining the porosity, the volume of the scaffolds was measured using the diameter and thickness of scaffolds. The weight of the scaffold was measured using a digital balance. Then, the density of scaffold (ρ_b) was obtained with the measured volume and mass. The porosity was calculated from the measured density and PCL density (ρ_p=1.145 g/cm^3) as below [30]:

$$\varepsilon = 1 - \frac{\rho_b}{\rho_p} \tag{5}$$

Water adsorption

The amount of water trapped by the scaffolds was determined as $\frac{w_2 - w_1}{w_1}$ where w_1 and w_2 are weight of dried scaffold and weight of soaked one in phosphate-buffered saline (PBS) overnight, respectively [31, 32]. In this analysis, scaffolds were cut in to 1×1 cm^2.

Degradation rate

Biodegradability of scaffolds was investigated with immersing them in 1 mg lysozyme/mL solution in PBS (pH = 7.4) for 1, 4, 7, 14, 21 and 28 days in an incubator at 37 ℃ [33]. Scaffolds were removed, washed 3 times with distilled water, dried and weighed (m_f). So, percentage of degradation (PD) was obtained from difference of weight ($m_i - m_f$) dividing to initial weight (m_i) [34].

MTT analysis

In our previous work [35], we differentiated hESCs to RPE cells and they were used in this study. To investigate cell viability and proliferation on different groups of scaffolds, cells were seeded on sterilized scaffolds at a density 5×10^4 cell /mL and 200 µL fresh medium was added to the plate. The groups were control (plate without scaffold, TCP), un-treated PCL scaffold (UPCL), hydrolyzed scaffold (HPCL), and plasma on the hydrolyzed scaffold (PHPCL). After 1, 4, and 7 days of incubation, media was removed from each well and 200 µL MTT was added and incubated in 37 ℃ and 5% CO$_2$ for 3-4 hours till purple formazan crystals were formed due to reduction of MTT by viable cells. Then, 200 µL DMSO was added in to each well to dissolve the formazan crystals and culture plates were shake in incubator for 20 min. After a while, absorbance of each well was read with a microplate reader at 570 nm [36, 37].

Scanning Electronic Microscopy (SEM)

In order to evaluate cell morphology on the scaffolds after 60 days, the medium was removed and scaffolds were fixed in 2.5% glutaraldehyde for 2 h. Next, samples were dehydrated through a series of graded ethanol solutions and dried in ambient air. Ultimately, the scaffolds were coated with gold and used for SEM [38].

Statistical analysis

In the present study, the data were presented as mean ± standard error of the mean (SEM). Each experiment was performed three times to be calculated by one-way analysis of variance (ANOVA) followed by Tukey's multi-comparison test to analyze the statistical difference (p < 0.01) between groups. In all tests, the significance level was set as p < 0.01.

RESULTS AND DISCUSSION
Scaffold fabrication and optimization

According to Table 2, the optimized diameter of the scaffold obtained by the ANFIS model was 110.5 nm. In the optimized situation, solution concentration and voltage were 0.065 g PCL /mL solvent and 18.9 kV, respectively. *Xiang et al.* used three different scaffolds (PCL, PCL/silk fibroin and PCL/silk fibroin/gelatin) to cultivate hESC-RPE cells that they had 157, 154 and 253 nm diameters, respectively [39]. In *Park et al.* study, the average diameter of nanofibers was reported as 2 µm, which is too high for AMD treatment [40].

The thickness of nanofibers was obtained 15±2 µm and the porosity was calculated 87%. *McHugh et al.* used porous polyester transwells and porous PCL as scaffolds. Their scaffolds had 64% and 90% porosity, respectively. Their results showed that scaffold porosity had a high effect on cell proliferation after eight weeks [41]. Also, in *Xiang et al.* study, porosity was calculated 85%, 87% and 90% for PCL, PCL/silk fibroin and PCL/silk fibroin/gelatin scaffolds, respectively [39].

Surface treatment and optimization

The contact angle for PCL scaffold without surface modification was measured as 120.33±2.06 degree, which shows the high hydrophobicity of this scaffold and the need for surface modification [39].

Time and concentration of alkaline hydrolysis analysis were optimized based on minimum contact angle (4.3 M

for the concentration of the alkaline solution and 104 mins for the time of immersing scaffold in alkaline solution). As shown in Table 2, alkaline hydrolysis reduced contact angle compared to the contact angle of un-treated PCL scaffolds, and the surface allowed a drop of water to spread out, which means hydrophilicity of the treated surface. Additionally, plasma radiation helps the scaffold to have a more water-friendly surface.

Guo et al. showed that alkaline hydrolysis treatment of porous poly (L-lactic acid) (PLLA) scaffolds decreases the water contact angle. So that, PLLA scaffold without surface treatment had an almost 80-degree water contact angle, and after treatment, it was reduced to 75 degrees [42].

Water adsorption

Calculation of water adsorption showed that with surface modification of scaffold, amount of hydrophilicity and water uptake would be increased. Hydrophilicity improves water adsorption of the scaffold, so the weight of the scaffold will be increased. Therefore, using two methods simultaneously for surface modification, having more hydrophilic groups, has more effect (Fig. 2). As shown in Fig. 2, surface treatment had a positive effect on the amount of water adsorption. So that, the PHPCL group modified by two types of method had a higher percentage of water adsorption. According to the statistical analysis, the difference between UPCL and other groups is significant at $P<0.001$ (#), and difference between HPCL and PHPCL is significant at $P<0.001$ (δ).

This was proved by the study of *Abedalwafa et al.*, which showed the amount of water adsorption would be increased by using surface modification [43]. In *Guo et al.* study, surface alkaline hydrolysis treatment of porous PLLA scaffold increases the water absorption rate, which indicates that the hydrophilicity of PLLA has been enhanced significantly [42].

Biodegradability

Fig. 2 shows that treating the surface of the scaffold leads to a high degradation rate during 28 days. So, using two types of modification seems to affect weight reduction due to increased hydrophilicity and higher water uptake (Fig 3). According to the Fig. 3, the weight of the scaffold will be decreased during 28 days. At first, since surface treatment is associated with weight reduction, the PHPCL group had the lowest weight comparing to HPCL and

Table 2: Contact angle for different groups of scaffolds.

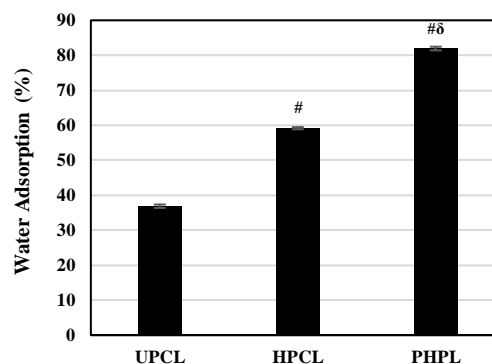| Groups of scaffolds	Contact angle (degree)
UPCL	120.33±2.06
HPCL	13.99±0.2
PHPCL	2.26±0.11

Fig. 2: Percentage of water adsorption for different groups of scaffolds. Accordingly, surface treatment increases the hydrophilicity and finally amount of water adsorption which is suitable for cell culturing. Difference between UPCL and other groups is significant at P<0.001 (#), and difference between HPCL and PHPCL is significant at P<0.001 (δ).

UPCL groups. Statistical analysis showed that the difference between UPCL and other groups is significant at $P<0.01$ (#) ,and difference between HPCL and PHPCL is significant at $P<0.001$ (δ).

Sant et al. used surface treatment for scaffolds made by PCL and PGS (2:1 ratio). It had a suitable effect on their degradation rate compare with scaffolds without surface modification. So, biodegradation in 0.1 mM concentration of the alkaline solution revealed 2-fold faster degradation of PCL-PGS scaffolds than untreated scaffolds [44].

Characterization of nanofibers and porosity

In Fig. 4, SEM images of all groups of scaffolds can be seen. By comparing the images, we can see that the surface treatment of PCL scaffolds directly affects fiber diameters. It can be observed that HPCL and PHPCL have a lower diameter in comparison with UPCL. Additionally, as shown by the circles, fibers of HPCL are more aligned and uniform compared to other groups. This difference help cells to have better adhesion, proliferation and finally make a layer
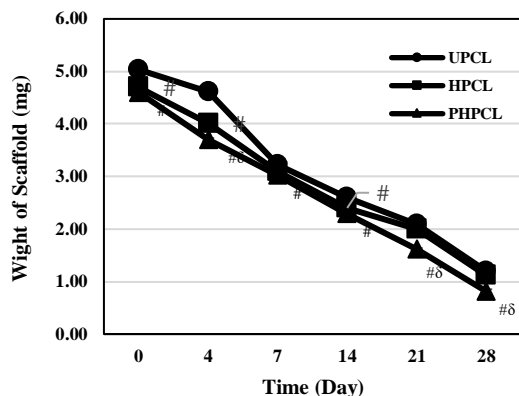
Fig. 3: Biodegradation rate of different groups of scaffolds. The weight of scaffolds were reduced during a month. Accordingly, surface modification has a positive effect on the degradation rate, which is vital in vivo. So that, PHPCL has higher biodegradability in comparison with HPCL. Difference between UPCL and other groups is significant at P<0.01 (#), and difference between HPCL and PHPCL is significant at P<0.001 (δ).
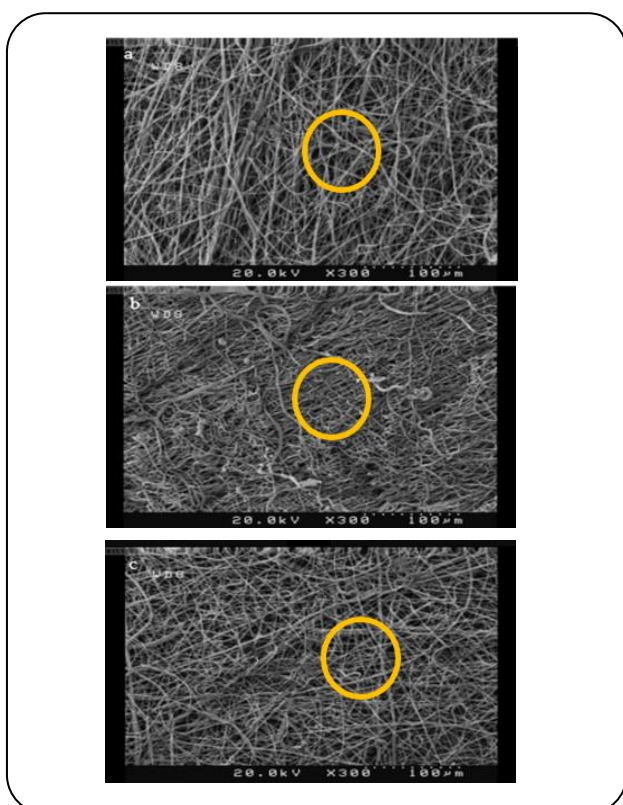

Fig. 4: SEM images of all groups of scaffolds. a) UPCL, b) HPCL and c) PHPCL. As shown by the circles, fibers of HPCL are more aligned and uniform in comparison to other groups. This difference help cells to have better adhesion, proliferation and finally make a layer.

In a study, it was demonstrated that surface hydrolysis of poly (glycolic acid) (PGA) meshes in 1N NaOH transformed ester groups on the surface of PGA fibers to carboxylic acid and hydroxyl groups and after hydrolysis, the fiber diameter of the polymer scaffold decreased. With the comparison of changes in fiber diameter and the hydrolysis time, their results showed that there is a linear relationship, with a rate of decrease in fiber diameter of 0.65 μm/min [45].

Biocompatibility

For investigation of cell viability and cell proliferation, MTT assay was used. As shown in Fig. 5, cell viability on TCP and UPCL scaffolds was lower than treated scaffolds. HPCL scaffold have a higher incretion in comparison with PHPCL group.

On the first day, all groups of scaffolds had a little more cell viability than TCP. Over the time, this difference became higher and the impact of using scaffolds for cell proliferation became apparent. According to the Fig. 5, using two types of surface modification simultaneously doesn't lead to higher cell viability and cell proliferation. This may be because excessive hydrophilicity of the scaffold's surface results in non-adhesion, thus compromising cell survival. So, it seems that HPCL group is a better choice for cell attachment, viability and proliferation. Based on the statistical analysis, the difference between TCP and other groups is significant at P<0.01 (*), the difference between UPCL and other groups is significant at P<0.001 (#), and the difference between HPCL and PHPCL is significant at P<0.001 (δ).

Similar studies with chondrocyte cells culturing on PCL scaffolds showed that surface modification (both hydrolysis and plasma) has suitable effects on cell proliferation after 21 days [46]. Also, *Park et al.* soaked PCL scaffolds in 1 N NaOH for an hour at room temperature and after preparation of scaffolds for cell seeding, osteoblast cells were cultured on scaffolds with and without surface modification. The results showed that treated PCL scaffolds, compared to untreated ones, had higher cell viability after 28 days. This tendency was because of the enhanced surface wettability and hydrophilicity of the surface-hydrolyzed fibrous scaffolds, which are the main contributors to induce the effective cell-scaffold interaction and cell growth [40].
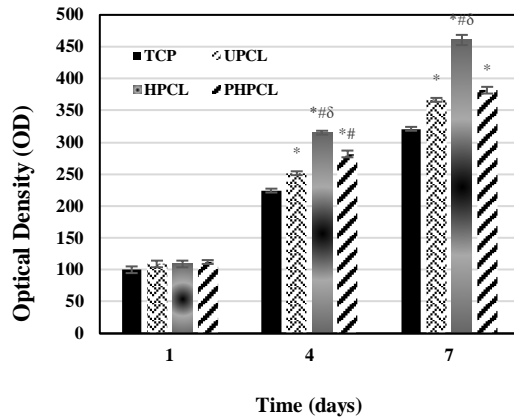
Fig. 5: 7 days MTT analysis of scaffolds. It can be seen that surface treatment had a positive effect on cell viability and cell proliferation. Moreover, the HPCL group had higher OD in comparison with the PHPCL group. The difference between TCP and other groups is significant at P<0.01 (*), the difference between UPCL and other groups is significant at P<0.001 (#), and the difference between HPCL and PHPCL is significant at P<0.001 (δ).
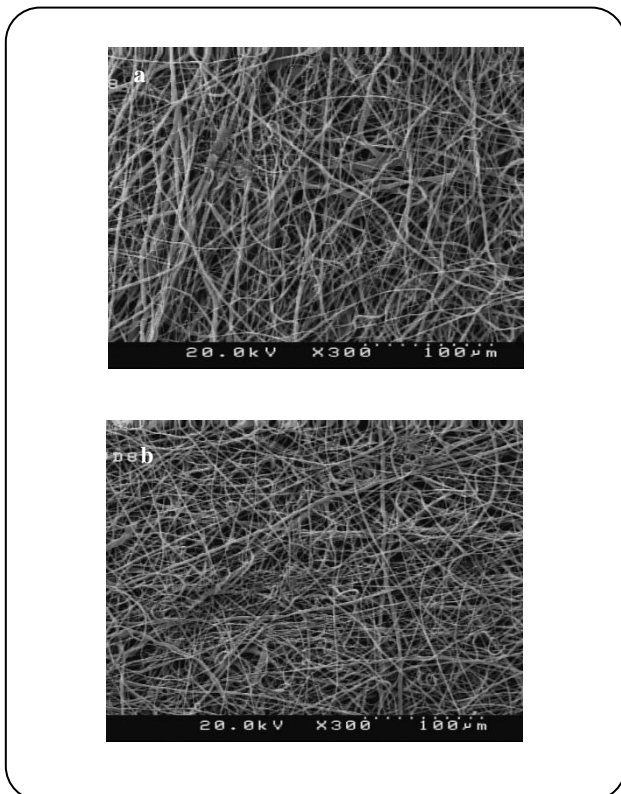

Fig. 6: No cell was seen in UPCL (a) and PHPCL (b) after 60 days by SEM. It seems that both groups are not good choices for cell proliferation and making a layer with the aim of AMD treatment.

Morphology and cell adhesion

In order to investigate cell morphology and adhesion on the surface of different groups of scaffolds, SEM images were prepared after 60 days. No cell was observed in UPCL and PHPCL (Fig. 5). As shown in Fig. 6, the cells not only keep their hexagonal (Fig. 6a) and stretched morphology after 60 days, but also microvilli on their surface is obvious in HPCL scaffolds (Fig. 6d). It means that the high hydrophobicity of UPCL scaffolds caused cell death. Additionally, using two kinds of surface treatment simultaneously increases surface hydrophilicity, which does not allow cells to adhere well. These findings were observed and proved in all three replications for all groups and only one of the SEM images of groups are shown in Fig. 6 and Fig. 7.

The effect of surface treatment (air plasma treated for 2 min at a power of 80 W) of commercially available polyurethanes was investigated by *Williams et al.* Morphological assessment of cells demonstrated that on the untreated substrates, the cells adhered to the surface were not well spread. While the cells on treated surfaces were well spread [47]. *Tezcaner et al.* studied the effect of the different situations of plasma radiation (100 W, 10 min and 100 W, 20 min) on cell culture of bed. During the first 4 h in culture, the cells that were just weakly attached to the beds had a round shape. They observed an improvement in the adhesion of RPE cells onto poly(hydroxybutyrate-co-hydroxy valerate) (PHBV) films after surface modification. Additionally, the percent of spread cells within a population was highest in 100 W, 10 min plasma treated films [36].

CONCLUSIONS

Electrospinning parameters of PCL scaffolds were optimized with a fuzzy model for the first time to reach minimum diameter. During the incorporation of scaffold for AMD treatment, cell adhesion and proliferation are the most critical parameters. To enhance the mentioned factors, surface treatment of PCL was performed. Water uptake, porosity, and biodegradability of treated scaffolds were increased significantly. Culturing hESC-RPE cells on all groups of scaffolds had different results. MTT analysis showed that UPCL had no significant difference with TCP. In contrast, treated scaffolds had better cell viability and proliferation during a week.
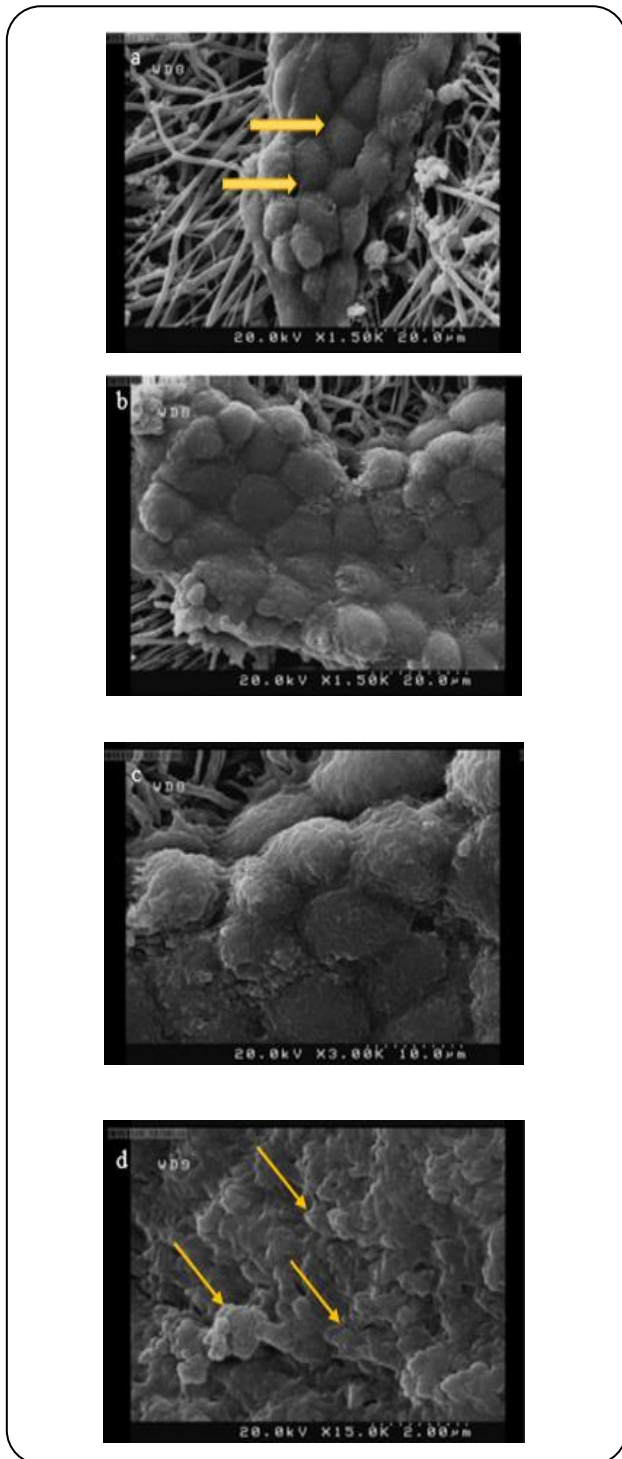
Fig. 7: a,b) Cell morphology and formation of RPE layer on HPCL scaffold. As shown by two arrows in (a), hESC-RPE cells have hexagonal morphology. Additionally, cell layer formation can be seen in (b). c, d) Microvilli of cells with different scales (10 µm and 2 µm, respectively) on HPCL scaffolds interestingly are able to be seen by three arrows in (d) in larger scale rather than (c).

Additionally, SEM images of cells on scaffolds showed that HPCL was the most suitable scaffold for cell proliferation after 60 days. The main reason we did not observe any cell on PHPCL is its high hydrophilicity of this scaffold leads to lower cell adhesion and cell viability. Based on the results, it seems that HPCL scaffolds can be a good choice for RPE cell attachment and proliferation, which can be used in AMD treatment.

REFERENCES

[1] Kashani A.H., Lebkowski J.S., Rahhal F.M., Avery R.L., Salehi-Had H., Dang W., Lin C.M., Mitra D., Zhu D., Thomas B.B., Hikita S.T., A Bioengineered Retinal Pigment Epithelial Monolayer for Advanced, Dry Age-related Macular Degeneration, *Sci. Transl. Med.*, **10**: eaao4097 (2018).

[2] Thomas B.B., Zhu D., Zhang L., Thomas P.B., Hu Y., Nazari H., Stefanini F., Falabella P., Clegg D.O., Hinton D.R., Humayun M.S., Survival and Functionality of hESC-derived Retinal Pigment Epithelium Cells Cultured as a Monolayer on Polymer Substrates Transplanted in RCS Rats, *Investig. Ophthalmol. Vis. Sci.*, **57**: 2877-2887 (2016).

[3] Sadda S.R., Guymer R., Holz F.G., Schmitz-Valckenberg S., Curcio C.A., Bird A.C., Blodi B.A., Bottoni F., Chakravarthy U., Chew E.Y., Csaky K., Consensus Definition for Atrophy Associated with Age-Related Macular Degeneration on OCT: Classification of Atrophy Report 3, *Ophthalmology*, **125**: 537-548 (2018).

[4] Mitchell P., Liew G., Gopinath B., Wong T.Y., Age-Related Macular Degeneration, *Lancet*, **392**: 1147-1159 (2018).

[5] Zadeh M.A., Khoder M., Al-Kinani A.A., Younes H.M., Alany R.G., Retinal Cell Regeneration Using Tissue Engineered Polymeric Scaffolds, *Drug Discov. Today*, **24**: 1669–1678 (2019).

[6] Hotaling N.A., Khristov V., Wan Q., Sharma R., Jha B.S., Lotfi M., Maminishkis A., Simon Jr C.G., Bharti K., Nanofiber Scaffold-Based Tissue-Engineered Retinal Pigment Epithelium to Treat Degenerative Eye Diseases, *J. Ocul. Pharmacol. Ther.*, **32**: 272–285 (2016).

[7] Di Foggia V., Makwana P., Ali R.R., Sowden J.C., Induced Pluripotent Stem Cell Therapies for Degenerative Disease of the Outer Retina: Disease Modeling and Cell Replacement, *J. Ocul. Pharmacol. Ther.*, **32**: 240-252 (2016).

[8] Shahmoradi S., Hatamian A.S., Tabandeh F., Yazdian F., Polycaprolacton as a Suitable Scaffold for Retina Diseases: Based on Statistical Analysis, (2015).

[9] Mazzilli J.L., Snook J.D., Simmons K., Domozhirov A.Y., Garcia C.A., Wetsel R.A., *et al.*, A Preclinical Safety Study of Human Embryonic Stem Cell-Derived Retinal Pigment Epithelial Cells for Macular Degeneration, *J. Ocul. Pharmacol. Ther.*, **36**: 65–69 (2020).

[10] Song W.K., Park K.M., Kim H.J., Lee J.H., Choi J., Chong S.Y., Shim S.H., Del Priore L.V., Lanza R., Treatment of Macular Degeneration Using Embryonic Stem Cell-derived Retinal Pigment Epithelium: Preliminary Results in Asian Patients, *Stem Cell Reports*, **4**: 860-872 (2015).

[11] Saatchi A.R., Seddiqi H., Amoabediny G., Helder M.N., Zandieh-Doulabi B., Klein-Nulend J., Computational Fluid Dynamics in 3D-Printed Scaffolds with Different Strand-Orientation in Perfusion Bioreactors, *Iran. J. Chem. Chem. Eng. (IJCCE)*, **39**: 307–320 (2020).

[12] Forest D.L., Johnson L. V., Clegg D.O., Cellular Models and Therapies for Age-Related Macular Degeneration, *DMM Dis. Model. Mech.*, **8**: 421-427 (2015).

[13] Croze R.H., Clegg D.O., Differentiation of Pluripotent Stem Cells into Retinal Pigmented Epithelium. In Cell-Based Therapy for Retinal Degenerative Disease, *Karger Publishers*, 81–96 (2014).

[14] Tan E.Y.S., Sing S.L., Yeong W.Y., "Scaffolds for Retinal Repairs. In Handbook of Tissue Engineering Scaffolds": Volume Two, (2019).

[15] Pennington B.O., Clegg D.O., Pluripotent Stem Cell-based Therapies in Combination with Substrate for the Treatment of Age-related Macular Degeneration, *J. Ocul. Pharmacol. Ther.*, (2016).

[16] Calejo M.T., Ilmarinen T., Jongprasitkul H., Skottman H., Kellomäki M., Honeycomb Porous Films as Permeable Scaffold Materials for Human Embryonic Stem Cell-derived Retinal Pigment Epithelium, *J. Biomed. Mater. Res. - Part A*, (2016).

[17] Calejo M.T., Haapala A., Skottman H., Kellomäki M., Porous Polybutylene Succinate Films Enabling Adhesion of Human Embryonic Stem Cell-derived Retinal Pigment Epithelial Cells (hESC-RPE), *Eur. Polym. J.*, (2019).

[18] Shahmoradi S., Yazdian F., Tabandeh F., Soheili Z.S., Hatamian Zarami A.S., Navaei-Nigjeh M., Controlled Surface Morphology and Hydrophilicity of Polycaprolactone Toward Human Retinal Pigment Epithelium Cells, *Mater. Sci. Eng. C*, **73**: 300-309 (2017).

[19] Hafizi A., Koolivand-Salooki M., Janghorbani A., Ahmadpour A., Moradi M.H., An Investigation of Artificial Intelligence Methodologies in the Prediction of the Dirty Amine Flow Rate of a Gas Sweetening Absorption Column, *Pet. Sci. Technol.*, **32**: 527-534 (2014).

[20] Qin X., Wu D., Effect of Different Solvents on Poly(caprolactone)(PCL) Electrospun Nonwoven Membranes, *J. Therm. Anal. Calorim.*, **107**: 1007-1013 (2012).

[21] Baker S.R., Banerjee S., Bonin K., Guthold M., Determining the Mechanical Properties of Electrospun Poly-ε-caprolactone (PCL) Nanofibers Using AFM and a Novel Fiber Anchoring Technique, *Mater. Sci. Eng. C*, **59**: 203-212 (2016).

[22] Shahmoradi S., Hatamina A.S., Yazdian F., Tabandeh F., Investigation and Optimization of Effective Parameters in Fabrication of Scaffolds with Electrospinning for Using in Retina, (2015).

[23] Jang J.S.R., ANFIS: Adaptive-Network-Based Fuzzy Inference System, *IEEE Trans. Syst. Man Cybern.*, (1993).

[24] Chang F.J., Chang Y.T., Adaptive Neuro-fuzzy Inference System for Prediction of Water Level in Reservoir, *Adv. Water Resour.*, **29**: 1-10 (2006).

[25] Anbazhagan S., Thiruvengatam V., Kulanthai K., Adaptive Neuro-Fuzzy Inference System and Artificial Neural Network Modeling for the Adsorption of Methylene Blue by Novel Adsorbent in a Fixed - Bed Column Method, *Iran. J. Chem. Chem. Eng. (IJCCE)*, **39**: 75–93 (2020).

[26] Davoody M., Abdul Raman A.A., Asgharzadeh Ahmadi S., Binti Ibrahim S., Parthasarathy R., Determination of Volumetric Mass Transfer Coefficient in Gas-Solid-Liquid Stirred Vessels Handling High Solids Concentrations: Experiment and Modeling, *Iran. J. Chem. Chem. Eng. (IJCCE)*, **37**: 195–212 (2018).

[27] Kosorn W., Thavornyutikarn B., Janvikul W., Effects of Surface Treatments of Polycaprolactone Scaffolds on their Properties, *Adv. Mat. Res.*, **747**: 178-181 (2013).

[28] Uppanan P., Thavornyutikarn B., Kosorn W., Kaewkong P., Janvikul W., Enhancement of Chondrocyte Proliferation, Distribution, and Functions within Polycaprolactone Scaffolds by Surface Treatments, *J. Biomed. Mater. Res. - Part A*, **103**: 2322-2332 (2015).

[29] Díaz E., Sandonis I., Valle M.B., In vitro Degradation of Poly (caprolactone)/nHA Composites, *J. Nanomater.*, **2014**: (2014).

[30] Sultana N., Wang M., Fabrication of HA/PHBV Composite Scaffolds through the Emulsion Freezing/freeze-drying Process and Characterisation of the Scaffolds, *J. Mater. Sci.: Mater. Med.,* **19**: 2555-2561 (2008).

[31] Zhu Y., Gao C., Shen J., Surface Modification of Polycaprolactone with Poly(methacrylic acid) and Gelatin Covalent Immobilization for Promoting its Cytocompatibility, *Biomaterials*, **23**: 4889-4895 (2002).

[32] Qi H., Ye Z., Ren H., Chen N., Zeng Q., Wu X., Lu T., Bioactivity Assessment of PLLA/PCL/HAP Electrospun Nanofibrous Scaffolds for Bone Tissue Engineering, *Life Sci.*, **148**: 139-144 (2016).

[33] Zhou Z.H., He S.L., Huang T.L., Liu L.H., Liu Q.Q., Zhao Y.M., Ou B.L., Zeng W.N., Yang Z.M., Cao D.F., Degradation Behaviour and Biological Properties of Gelatin/hyaluronic Acid Composite Scaffolds, *Mater. Res. Innov.*, **17**: 420–424 (2013).

[34] Cummins K.A., Lee K.L., Cooper J.A., "Quantification of Entrapped Model Protein Released during Electrospun Nanofiber Degradation", 2015 41st *Annual Northeast Biomedical Engineering Conference,* NEBEC (2015).

[35] Zahabi A., Shahbazi E., Ahmadieh H., Hassani S.N., Totonchi M., Taei A., Masoudi N., Ebrahimi M., Aghdami N., Seifinejad A., Mehrnejad F., A New Efficient Protocol for Directed Differentiation of Retinal Pigmented Epithelial Cells from Normal and Retinal Disease Induced Pluripotent Stem Cells, *Stem Cells Dev.*, **21**: 2262-2272 (2012).

[36] Tezcaner A., Bugra K., Hasirci V., Retinal Pigment Epithelium Cell Culture on Surface Modified Poly(hydroxybutyrate-co-hydroxyvalerate) Thin Films., *Biomaterials*, **24**: 4573–4583 (2003).

[37] Gautam S., Dinda A.K., Mishra N.C., Fabrication and Characterization of PCL/gelatin Composite Nanofibrous Scaffold for Tissue Engineering Applications by Electrospinning Method, *Mater. Sci. Eng. C*, **33**: 1228–1235 (2013).

[38] Thumann G., Viethen A., Gaebler A., Walter P., Kaempf S., Johnen S., Salz A.K., The In vitro and In vivo Behaviour of Retinal Pigment Epithelial Cells Cultured on Ultrathin Collagen Membranes, *Biomaterials*, **30**: 287-294 (2009).

[39] Xiang P., Wu K.C., Zhu Y., Xiang L., Li C., Chen D.L., Chen F., Xu G., Wang A., Li M., Jin Z.B., A novel Bruch's Membrane-mimetic Electrospun Substrate Scaffold for Human Retinal Pigment Epithelium Cells, *Biomaterials*, **35**: 9777-9788 (2014).

[40] Park J.S., Kim J.M., Lee S.J., Lee S.G., Jeong Y.K., Kim S.E., Lee S.C., Surface Hydrolysis of Fibrous Poly(ε-caprolactone) Scaffolds for Enhanced Osteoblast Adhesion and Proliferation, *Macromol. Res.*, **15**: 424-429 (2007).

[41] McHugh K.J., Tao S.L., Saint-Geniez M., Porous Poly(ε-caprolactone) Scaffolds for Retinal Pigment Epithelium Transplantation, *Investig. Ophthalmol. Vis. Sci.*, **55**: 1754-1762 (2014).

[42] Guo C., Cai N., Dong Y., Duplex Surface Modification of Porous Poly (lactic acid) Scaffold, *Mater. Lett.*, **94**: 11–14 (2013).

[43] Abedalwafa M., Wang F., Wang L., Li C., Biodegradable Poly-epsilon-caprolactone (PCL) for Tissue Engineering Applications: A review, *Rev. Adv. Mater. Sci.*, **34**: 123-140 (2013).

[44] Sant S., Iyer D., Gaharwar A.K., Patel A., Khademhosseini A., Effect of Biodegradation and De Novo Matrix Synthesis on the Mechanical Properties of Valvular Interstitial Cell-seeded Polyglycerol Sebacate–Polycaprolactone Scaffolds, *Acta Biomater.*, **9**: 5963–5973 (2013).

[45] Gao J., Niklason L., Langer R., Surface Hydrolysis of Poly(glycolic acid) Meshes Increases the Seeding Density of Vascular Smooth Muscle Cells, *J. Biomed. Mater. Res.*, **42**: 417-424 (1998).

[46] Janvikul W., Uppanan P., Thavornyutikarn B., Kosorn W., Kaewkong P., Effects of Surface Topography, Hydrophilicity and Chemistry of Surface-treated PCL Scaffolds on Chondrocyte Infiltration and ECM Production, *Procedia Eng.*, **59**: 158-165 (2013).

[47] Williams R.L., Krishna Y., Dixon S., Haridas A., Grierson I., Sheridan C., Polyurethanes as Potential Substrates for Sub-retinal Retinal Pigment Epithelial Cell Transplantation., *J. Mater. Sci. Mater. Med.*, **16**: 1087–1092 (2005).